Supramolecular Host–Inhibited Excited-State Proton Transfer and Fluorescence Switching of the Anti-Cancer Drug, Topotecan

ARTICLE *in* CHEMPHYSCHEM · OCTOBER 2013

Impact Factor: 3.42 · DOI: 10.1002/cphc.201300461 · Source: PubMed

4 AUTHORS, INCLUDING:

Krishna Gavvala
Indian Institute of Science Education and R…
25 PUBLICATIONS **75** CITATIONS
SEE PROFILE

Raj kumar Koninti
Indian Institute of Science Education and R…
15 PUBLICATIONS **44** CITATIONS
SEE PROFILE

Partha Hazra
Indian Institute of Science Education and R…
52 PUBLICATIONS **997** CITATIONS
SEE PROFILE

ChemPubSoc Europe

DOI: 10.1002/cphc.201300461

Supramolecular Host-Inhibited Excited-State Proton Transfer and Fluorescence Switching of the Anti-Cancer Drug, Topotecan

Krishna Gavvala, Abhigyan Sengupta, Raj Kumar Koninti, and Partha Hazra*[a]

The effect of cucurbit[7]uril (CB[7]) nano-caging on the photophysical properties, particularly excited-state proton transfer (ESPT) reaction, of an eminent anti-cancer drug, topotecan (TPT), is demonstrated through steady-state and time-resolved fluorescence measurements. TPT in water (pH 6) exists exclusively as the cationic form (C) in the ground state. However, the drug emission mainly comes from the excited-state zwitterionic form (Z*) of TPT, and is attributed to water-assisted ESPT between the 10-hydroxyl group and water, which leads to the transformation of C* to Z* of TPT. In the presence of CB[7], it is found that selective encapsulation of the C form of TPT results in the formation of a 1:1 inclusion complex (CB[7]:TPT), and the ESPT process is inhibited by this encapsulation process. As a result, C* becomes the dominant emitting species in the presence of CB[7] rather than Z*, and fluorescence switching takes place from green to blue. Time-resolved studies also support the existence of CB[7]-encapsulated cationic species as the major emitting species in the presence of the macrocyclic host. Semi-empirical quantum chemical calculations are employed to gain insight into the molecular picture of orientation of TPT in the inclusion complex. It is clearly seen from the optimised structure of 1:1 CB[7]:TPT inclusion complex that both 10-hydroxyl and 9-dimethylaminomethylene groups of TPT lie partly inside the cavity, and thereby inhibit the excited-state transformation of C* to Z* by the ESPT process. Finally, controlled release of the drug is achieved by means of fluorescence switching by introducing NaCl, which is rich in cells, as an external stimulus.

1. Introduction

Topotecan (TPT) is a water-soluble analogue of camptothecin (CPT), a pentacyclic alkaloid, which was first isolated by Wall et al. in 1966 from a Chinese tree *Camptotheca acuminata*, and has been clinically evaluated as an effective anti-cancer agent.[1] CPT and its water-soluble derivatives inhibit the activity of topoisomerase I enzyme through the formation of a cleavable enzyme–drug–DNA ternary complex, and thereby prevent important intracellular processes such as replication, transcription and repair.[2] Compared with CPT, TPT has a higher solubility in water and it also shows inhibitory activity against a broad spectrum of animal and human tumours.[3] The basic structure of TPT consists of five fused rings; among them, four are six-membered and one is five-membered (Scheme 1). TPT contains an additional hydroxyl group at the 9-position and a dimethylaminomethylene group at the 10-position on the quinoline moiety of CPT. The presence of these two functional groups causes this molecule to exhibit different photophysical properties in the excited state compared with CPT, and recently this molecule has received burgeoning interest from researchers working in the photophysical field.[4] The photophysics of TPT in solution has been mainly studied by UV/Vis absorption and fluorescence spectroscopic techniques.[4d,e] It was observed that under physiological conditions (pH 7), the drug exists in equilibrium between the enol (E), cationic (C) and zwitterionic (Z) forms in the ground state (Scheme 1).[4e] At lower pH, ground-state equilibrium exists between three different cationic species; on the other hand at higher pH, only anionic (A) species prevail.[4b] The presence of several protophilic and protophobic functional groups (10-hydroxyl group, quinoline nitrogen, 9-dimethylaminomethylene etc.) is responsible for the existence of different forms of TPT at different pH values. Although in the ground state the drug exists in different forms (E, C and Z) at physiological pH, TPT exhibits a single fluorescence peak in aqueous solution responsible for the emission from Z*, which is believed to be an outcome of excited-state proton transfer (ESPT).[4d,e] It is also found that the proton-

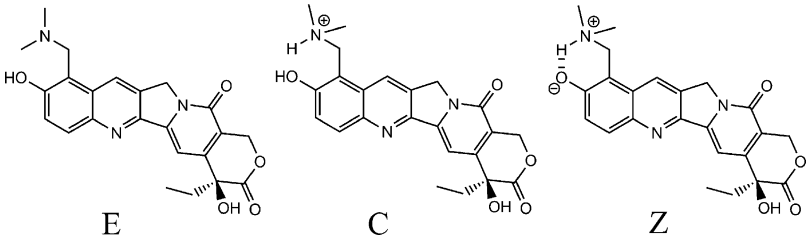

Scheme 1. Different forms of TPT that exist in aqueous solution.

[a] *K. Gavvala, A. Sengupta, R. K. Koninti, Dr. P. Hazra*
Department of Chemistry, Mendeleev Block
Indian Institute of Science Education and Research
Pune 411008, Maharashtra (India)
Fax: (+91) 20-25899790
E-mail: p.hazra@iiserpune.ac.in

Supporting information for this article is available on the WWW under http://dx.doi.org/10.1002/cphc.201300461.

transfer process in TPT is sensitive to polarity,[4e] and hence the excited-state photophysics of TPT can be modulated inside the nano-cavities of a supramolecular host, such as cyclodextrin, calixarene, cucurbituril and so forth. Although it has been shown that the stability of the drug could be improved by encapsulating the drug molecule into liposomes, cyclodextrins and calixarene,[5] no focus has been made on modulating the proton-transfer process of TPT inside those nano-cavities.

Like CPT derivatives, the anti-tumour activity of TPT is believed to be mainly dependent on the stability of the α-hydroxylactone moiety, which hydrolyses predominantly at physiological pH 7.4, and converts to the inactive carboxylate form.[5a] It was found that hydrolysis of the active lactone part of CPT can be 200 times faster in the presence of human serum albumin (HSA), because of the high binding affinity of the carboxylate form towards HSA.[6] On the other hand, the TPT hydrolysis rate is almost unperturbed by the presence of serum albumin protein in blood, and thereby favours anticancer activity of TPT relative to CPT.[7] Although the presence of HSA makes no change in the cytotoxic activity of TPT,[7] its rate of hydrolysis from the active lactone to inactive carboxylate form needs to be inhibited to use TPT as an effective anticancer drug.

In continuation of this effort, researchers observed that the stability of the lactone moiety could be improved by encapsulating the drug molecule into liposomes and cyclodextrins.[5] The results suggest that the solubility, stability and bio-availability of the drug are enhanced upon encapsulation compared with its free form.[5] However, to our knowledge, there is no such study available on the stability, topology and excited-state photophysics of the TPT drug upon interaction with cucurbituril. Cucurbit[*n*]uril (CB[*n*]) formed by acid-catalysed condensation of *n* glycoluril units with formaldehyde recently appeared as a promising macrocyclic container. Moreover, current reports about the non-toxic behaviour of CB[*n*] provide a boost for the use of CB[*n*] as a potential drug-delivery vehicle.[8] The pumpkin-shaped CB[*n*] is a macrocyclic compound that provides different cage diameters ranging from 4.5 to 12.5 Å for CB[5] to CB[10], respectively, and hence guest molecules of various sizes can be encased by the CB[*n*] the cavity.[9] The internal hydrophobic cavity is responsible for the complexation with guest molecules by hydrophobic interactions, whereas the two portals of CB[*n*] lined by ureido carbonyl groups give an extra stability through ion–dipole and/or hydrogen-bonding interactions.[9,10] Herein, we report the effect of confinement by CB[7] on the photophysics of TPT with the help of steady-state and time-resolved fluorescence spectroscopic techniques. The focus of this work is to characterise and compare the effect of nano-confinement on the ESPT process, which is the dominant photophysics observed in aqueous solution. Astonishingly, we have observed that the ESPT of TPT is inhibited inside the nano-cavity of CB[7]. Semi-empirical quantum chemical calculations have been employed in deciphering the molecular pictures of the interactions between TPT and CB[7].

2. Results and Discussion

Steady-State Observations

All the studies of TPT in the absence and presence of CB[7] were carried out in aqueous solution of pH 6 (Figure 1a). The choice of pH 6 is based on the fact that the lactone structure dominates at pH ≤ 6.[5a] To avoid the carboxylate form of TPT,

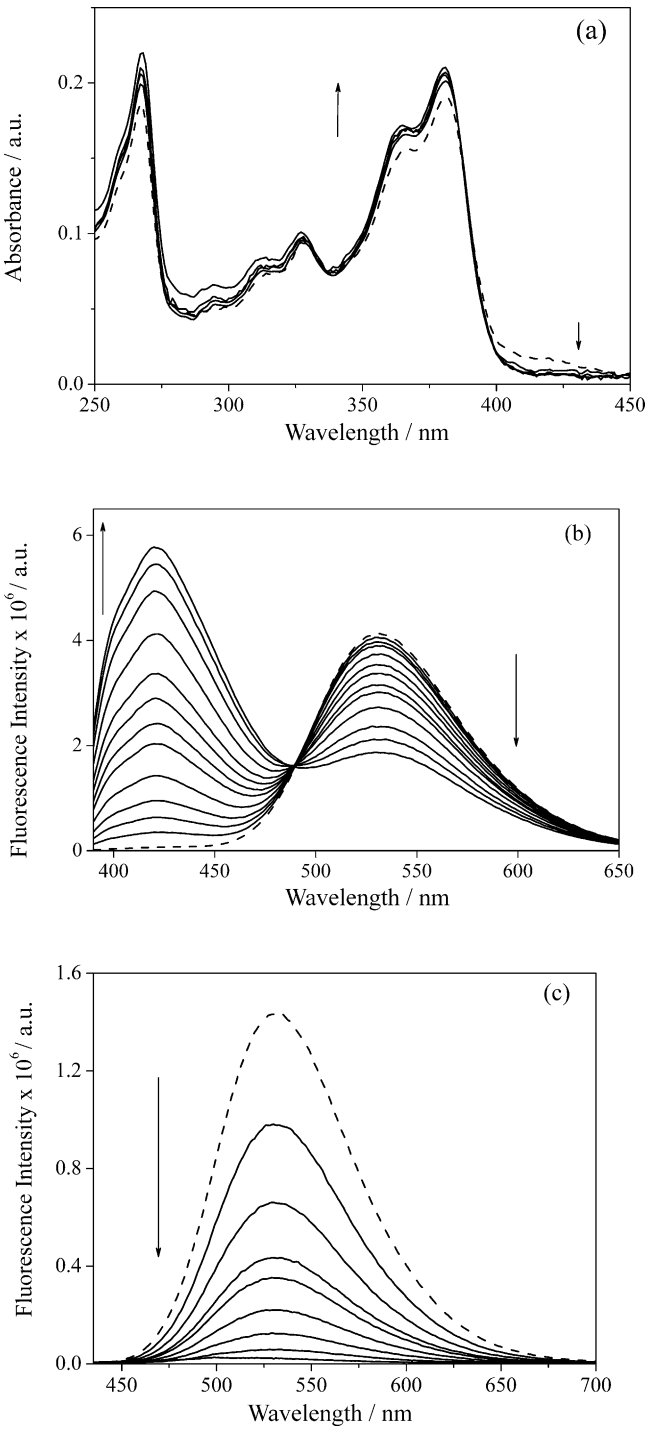

Figure 1. a) Absorption and b,c) emission spectra of TPT (8 μM) in the presence of CB[7] (0–1 mM, in the direction of the arrow) exciting at b) 380 and c) 410 nm. Dashed lines represent TPT in water.

which leads to toxicity, all the present work was performed near neutral pH. The absorption spectrum of TPT in water (pH 6) exhibits maxima between 350 and 400 nm, which are mainly a result of the π–π^*-type absorption of the quinoline moiety.[4e]

Considering the pK_a (6.5) of deprotonation of the 10-hydroxyl group and the pK_a (10.7) of the protonated 9-dimethylaminomethylene group,[11] we believe that the drug mainly exists as the cationic (C) form in aqueous medium of pH 6. The minute population of the Z form of the drug is reflected by the slight absorption of the drug at approximately 410 nm, and is attributed to the above-mentioned pK_a values. On addition of CB[7] to the TPT solution, absorption at 365 and 381 nm increases whereas absorption at 410 nm drops (Figure 1 a). The rise in absorbance of the former two peaks indicates an increasing population of C species in the presence of CB[7], whereas the decrement of absorption at 410 nm infers that the population of the Z form decreases compared with an aqueous solution of pH 6. In summary, these substantial changes in absorption spectra provide a preliminary notion of TPT–CB[7] interaction. To elucidate the mechanism of interaction and stoichiometry, we further employed steady-state and time-resolved emission measurements to divulge specific details of this interaction, which is discussed below.

The emission profiles of TPT in water (pH 6) and in the presence of CB[7] upon excitation at 375 nm are shown in Figure 1 b. In the absence of CB[7], the emission spectrum exhibits a single broad peak at 530 nm, which originates from the excited-state zwitterionic form (Z*) of TPT. This is because the Z* form of TPT is the main emitting species in water (pH 6.25), whereas the fluorescence from C* is not detectable in water.[4e] Here it is pertinent to mention that although the outcome fluorescence is from Z*, the C form of the drug is selectively excited at 375 nm. This can be attributed to the ESPT process by which water-assisted deprotonation of the 10-hydroxyl group takes place, and leads to the formation of the Z* form of the drug from C*. Therefore, we believe that the excited-state conversion of C* to Z* is the dominating photophysics in aqueous solutions of near neutral pH (pH 6). To further confirm this finding, we collected the emission profile of the drug at pH 3 (Figure S1 in the Supporting Information), at which the drug mainly exists as the C form, and we found a similar observation to that at pH 6. This further supports our conjecture that C* to Z* conversion is the major photophysics in aqueous solutions of pH 6. In polar aprotic and non-polar solvents, the emission from Z* is not detectable at all (Figure S2), which is ascribed to the absence of intermolecular hydrogen bonds between the solvent and 10-hydroxyl group in these solvents. Similar kinds of observations are also reported in the case of 10-hydroxycamptothecin, and it has been inferred that the ESPT is the main excited-state photophysics of 10-hydroxycamptothecin in water.[12]

The fluorescence spectra of TPT in the presence of CB[7] display a striking feature. By gradual addition of CB[7], the emission peak intensity at 530 nm reduces and a new blue-shifted peak at 425 nm develops progressively (Figure 1 b). At higher CB[7] concentration, the 425 nm peak is almost saturated, whereas the intensity at 530 nm is drastically reduced. These substantial changes in the emission profiles (Figure 1 b) confirm the strong interaction between TPT and CB[7]. As the 530 nm peak originates from Z*, the decrease in peak intensity at 530 nm reflects that the formation of the zwitterion is becoming inhibited by the presence of CB[7]. The new peak at 425 nm in the presence of CB[7] may be attributed to either the C* or E* form of the drug. However, at pH 6 the population of the C form dominates over the E form. Moreover, if the C form of the drug binds with CB[7], then it will have additional binding strength through ion–dipole interaction.[9,10,13] On the other hand, binding of the E form involves only weak hydrophobic interaction, and hence the binding affinity of the E form will be much weaker than that of the C form. Therefore, we believe that the C form of the drug binds preferentially with CB[7] and emits blue fluorescence at 425 nm. Inside the CB[7] cavity ESPT from the 10-hydroxyl group of TPT to water ceases, and therefore CB[7]-bound C forms of the drug are not able to transform to Z* in the excited state. Another possibility is that the pK_a of the hydroxyl group of the drug undergoes an upward shift upon binding with CB[7], and subsequently reduces the excited-state transformation drift to Z*.

To verify the latter possibility, we adopted pH titration methods to find out the pK_a value of the phenol OH group in the ground as well as excited states by using absorption and fluorescence measurements, respectively (Figure S3).[13] Here it is relevant to mention that in the absence of CB[7], the reported pK_a values of the phenol OH group in the ground and excited states are 6.5 and -2.62, respectively, and this large decrease in pK_a value ($\Delta pK_a = pK_a - pK_a^* = 9.12$) is solely responsible for exhibiting the ESPT phenomenon in the excited state. It has been well documented in the literature that the pK_a value of a guest molecule increases inside the CB[7] cavity due to electron-rich carbonyl portals of CB[7].[13,14] Similarly, in the present case both pK_a and pK_a* values of TPT in the presence of CB[7] increase from 6.5 to 7.05 and -2.62 to 5.51, respectively (Figure S3). Therefore, the decrease in ΔpK_a from 9.12 to 1.54 in the presence of CB[7] may be one of the plausible reasons for inhibition of the ESPT of TPT. In either of the cases, the excited-state equilibrium between C* and Z*, which is the dominant excited-state photophysics in normal aqueous medium, is inhibited by encapsulation of the C form of the drug by CB[7]. With each addition of CB[7], the equilibrium shifts more towards C*, and therefore the peak intensity corresponding to C* progressively increases. To substantiate that the ESPT process is inhibited by the presence of CB[7], we also monitored the emission profiles of TPT by selectively exciting the Z form of the drug at 410 nm with increasing concentration of host (Figure 1 c). It was observed that the peak intensity at 530 nm decreases progressively with gradual addition of CB[7]. This observation further confirms that the Z* population of TPT is decreased by selective incorporation of the C form of the drug inside the nano-cavity of the CB[7] host.

Now, it is necessary to find out whether the reduced polarity and/or lack of hydrogen-bonding network of water are (is) responsible for the existence of C* instead of Z* inside the CB[7] nano-cavity. To verify the above-mentioned effects on the ex-

cited-state photophysics of TPT, the emission profiles were probed in both dioxane/water and MeCN/water binary mixtures excited at 375 nm (Figure 2). Acetonitrile is chosen considering the fact that it is a polar aprotic solvent having a solvent polarity parameter $E_T(30)$ of 45.6. Dioxane is chosen because it is considered as a non-polar solvent (having $E_T(30)$ of 36.0)[15] and at the same time it can act as a Lewis base.[16] Therefore, both MeCN and dioxane can stabilise cationic species. It is observed that the emission from Z* (at 530 nm) dominates at higher percentage of water, whereas the emission from C* (at ≈425 nm) dominates at higher percentage of MeCN or dioxane (Figure 2). As C* is the main emitting species in both MeCN and dioxane (although their polarity is hugely different), we believe that the polarity of the solvent does not have a major role in stabilising the Z* form of TPT, but rather the hydrogen-bonding network of the solvent is the major contributing factor. Our observation is also supported by literature reports in which it has been documented that zwitterionic forms exist in hydrogen-bonded solvents, such as methanol, ethanol and water.[17] The inhibition of Z* formation tendency inside the CB[7] cavity is further supported by excitation spectra collected at two distinct peak maxima (425 and 530 nm) observed in the emission spectra (see Note S1 and Figure S4).

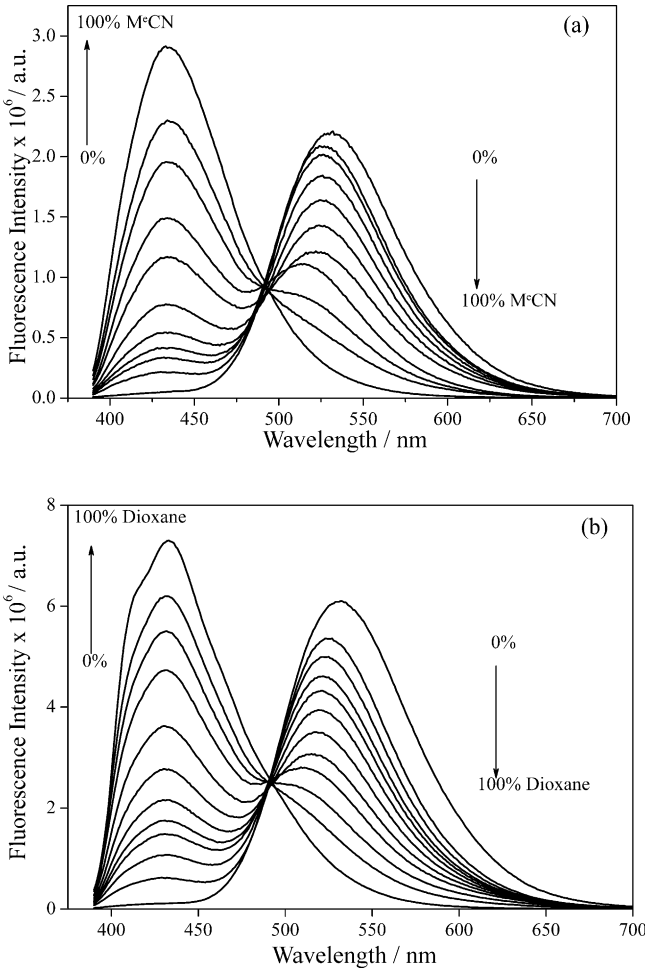

Figure 2. Emission profiles of TPT in a) MeCN/water and b) dioxane/water mixtures monitored at $\lambda_{ex} = 380$ nm.

The stoichiometry and apparent binding constant for the inclusion complexes are calculated by using a non-linear version of the Benesi–Hildebrand plot [Eq. (1)]:[18]

$$F/F_0 = 1 + (F_1/F_0 - 1)\left(\frac{[CB[7]]K}{1 + [CB[7]]K}\right) \quad (1)$$

in which F_0 and F are fluorescence intensities of TPT in the absence and presence of CB[7], respectively, and F_1 is the fluorescence intensity of TPT:CB[7] inclusion complex. The non-linear fitting shows 1:1 inclusion complexation between TPT and CB[7], and the association constant (K_1) is estimated to be $(5000 \pm 150)\ M^{-1}$ (Figure 3a). The 1:1 stoichiometry of the TPT:CB[7] complex is further confirmed by Job's plot (Figure 3b). Moreover, the value of free energy change ($\Delta G^\circ = -21.25\ kJ\,mol^{-1}$ at 298 K) for the formation of the inclusion complex infers that the complexation process is energetically feasible at room temperature. Notably, the population of Z* does not completely disappear even at 1 mM host concentration, as the 530 nm peak still exists at the above-mentioned

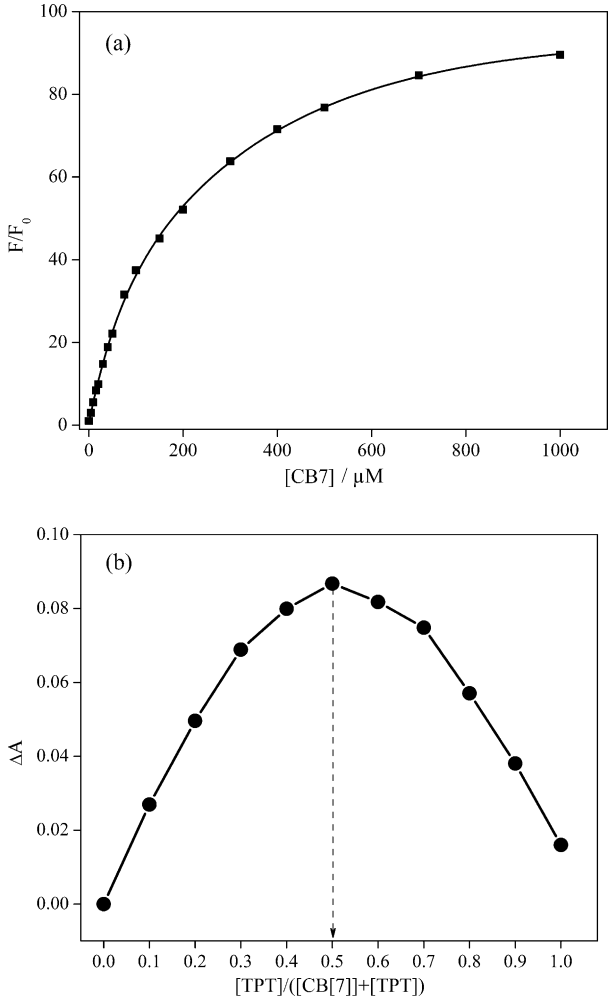

Figure 3. a) Non-linear regression analysis using Equation (1). b) Job's plot constructed from the absorbance changes ΔA at 380 nm.

host concentration. As there is no shift in emission maximum of Z*, we can rule out the possibility that Z* is encased by CB[7]. The value of the binding constant also indicates that approximately 15% of TPT does not form an inclusion complex with CB[7]. However, there is a possibility that some Z* population might be involved in the formation of an exclusion complex with CB[7], and this will be verified through time-resolved studies.

On comparison of this observation with previous reports, we did not find any literature related to fluorescence switching as a detection of ESPT blockage. In most of the cases, we found an increase of proton transfer in biological as well as bio-mimicking confined media.[19] Moreover, research work involving proton transfer in the CB[7] inclusion complexes is scarcely available. Recently, Shaik et al. observed that ESPT of 2-(2′-hydroxyphenyl)benzimidazole is partially restricted inside the CB[7] cavity as the acidic nature of the phenolic group reduces, though fluorescence switching was not observed in their system.[19d] In the present work, we observed that ESPT of TPT is completely restricted inside the CB[7] cavity resulting in fluorescence switching from green to blue colour.

Time-Resolved Emission Measurements

Lifetime Measurements

Time-resolved fluorescence lifetime measurement is an excellent tool to monitor the dynamics of molecules in the excited state, and is a sensitive technique in identifying multiple emissive species present in a system.[20] Decay profiles of TPT in the absence and presence of CB[7] were collected at 425 and 530 nm (exciting at 375 nm) to monitor both excited-state cationic species (C*) and zwitterionic species (Z*), respectively. Fluorescence transients are shown in Figure 4 and the results are presented in Tables 1 and 2. The decay profile collected at 425 nm in aqueous solution of TPT is very fast, and close to the response time of our time-correlated single photon counting setup. However, after deconvolution we were able to detect a fluorescence lifetime component of approximately 40 ps, which may be attributed to the fluorescence lifetime and/or deprotonation time of the C form of TPT. In the presence of CB[7], a long component (≈2 ns) appears in the decay profile along with an approximately 40 ps component, and the contribution of the long component increases progressively with the gradual addition of host (Table 1). This newly detected component is likely to be an outcome of interaction between the C form of TPT and CB[7]. It is already evident from the emission spectra that the population of C* is enhanced in the presence of CB[7] due to the suppression of the transformation

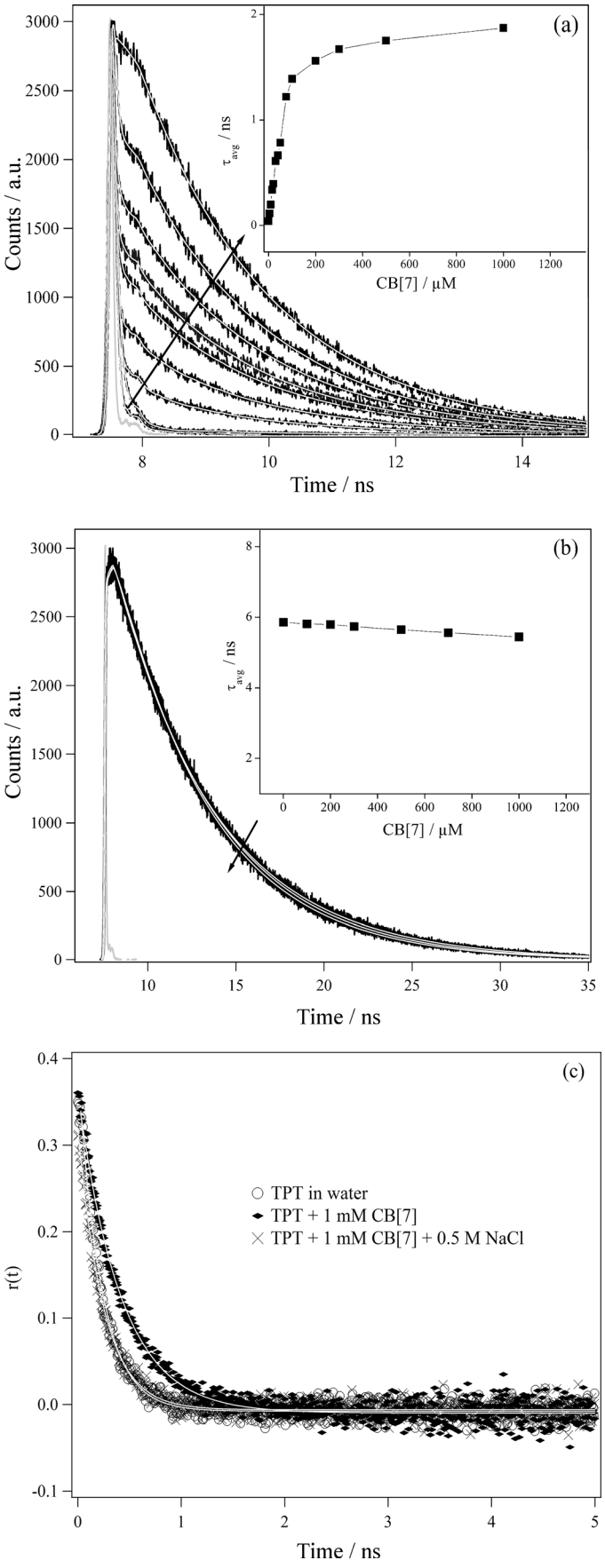

Figure 4. Fluorescence and anisotropy decay transients of TPT (8 μM) in the presence of CB[7] (0–1 mM, in the direction of the arrow). a,b) Fluorescence decay profiles monitored at 425 and 530 nm, respectively (the inset shows the fluorescence lifetime of TPT versus concentration of CB[7]). The lamp profile is denoted by a grey line in both (a) and (b). c) Anisotropy decay profiles of TPT in the absence (monitored at 530 nm) and presence of CB[7] (monitored at 425 nm) as well as CB[7] containing 0.5 M NaCl (monitored at 530 nm) as an external stimulus.

Table 1. Fluorescence decay transients of TPT (8 μM) in the absence and presence of CB[7] collected at 425 nm.

Concentration of CB[7] [μM]	τ_1	τ_2	a_1	a_2	τ_{avg}[a]	χ^2
0	0.041	–	1	–	0.041	1.1
4	0.042	1.95	0.96	0.04	0.113	1.03
9	0.042	2.03	0.92	0.08	0.196	1.02
15	0.049	2.11	0.86	0.14	0.337	1.05
20	0.046	2.11	0.83	0.17	0.393	1.01
30	0.054	2.15	0.73	0.27	0.61	0.99
40	0.051	2.09	0.7	0.3	0.663	1.05
50	0.052	2.12	0.65	0.35	0.784	0.99
75	0.076	2.13	0.44	0.56	1.22	0.99
100	0.072	2.16	0.37	0.63	1.39	1.04
200	0.09	2.1	0.27	0.73	1.56	1.06
300	0.07	2.088	0.21	0.79	1.67	1.06
500	0.072	2.1	0.18	0.82	1.75	1.07
1000	0.07	2.12	0.12	0.88	1.87	0.99

[a] $\tau_{avg} = (a_1\tau_1 + a_2\tau_2)$.

Table 2. Fluorescence decay transients of TPT (8 μM) in the absence and presence of CB[7] collected at 530 nm.

Concentration of CB[7] [μM]	τ	χ^2
0	5.85	1.05
100	5.81	1.09
200	5.79	1.06
300	5.73	0.99
500	5.64	1.02
700	5.56	1.02
1000	5.44	1.12

pathway from C* to Z* inside the nano-cavity of CB[7]. Moreover, it was found that the cationic species has a longer fluorescence lifetime in polar aprotic and non-polar solvents than in water, which abstracts the proton from the 10-hydroxyl group and facilitates the conversion to the Z* form of TPT (Table S2). Hence, the long lifetime of C* is attributed to the absence of a hydrogen-bonding network inside the CB[7] cavity, and infers that an intermolecular hydrogen-bonding network with solvents has a pivotal role for the stability of the C form of TPT. With the gradual addition of CB[7], the contribution of the long-lifetime component is enhanced progressively, and becomes a major component (≈80%) at higher concentrations of host (>300 μM).

This observation suggests the dominating existence of the encapsulated C form along with a minute population of the free C form of TPT at higher CB[7] concentration. The average lifetime increases steadily with the concentration of CB[7] (Figure 4a, inset). We also performed the same experiment in acidic solutions (pH 3). The fluorescence decay fitting parameters are summarised in Table S1. The results are found to be same as those for pH 6. These observations clearly support our conjecture that CB[7] mainly interacts with cationic TPT and the resulting complex is stabilised by ion–dipole interaction. Therefore, the lifetime results validate our steady-state observation, for which we found a strong rise of the 425 nm emission corresponding to the formation of a 1:1 inclusion complex between the C form of TPT and CB[7]. We believe that the selective insertion of the C form of TPT inside the CB[7] cavity keeps the molecule away from water and enhances the fluorescence intensity as well as lifetime of the C form of the drug. To gain insight into the dynamics of the excited-state zwitterion form (Z*) of TPT in the absence and presence of CB[7], we also monitored the decay profile of the drug at 530 nm, as the emission at 530 nm is mainly characterised by the Z* form of TPT. Zwitterionic species exhibit a long lifetime of approximately 5.85 nm in aqueous solution at near neutral pH (pH 6). In the presence of CB[7], the fluorescence lifetime does not change drastically; however, a slight reduction of the lifetime of Z* (Figure 4b, inset), observed at higher concentration of host, manifests that the Z form of TPT is not encaged by CB[7]. The slight reduction in lifetime might be attributed to the hydrogen-bonding interaction between Z* and carbonyl groups of the CB[7] portal, as it has been observed that hydrogen-bonding interaction sometimes reduces the excited-state lifetime of a fluorophore.[21]

Anisotropy Measurements

To obtain information about the rotational motion of the drug in solution and the restriction imposed by the microenvironment around the probe, we performed time-resolved anisotropy measurements. The anisotropy decays of TPT in the absence and presence of CB[7] are shown in Figure 4c. Anisotropy decays are fitted by Equation (2):[20a]

$$r(t) = r_0 \sum f_i \exp(-\frac{t}{\tau_{ri}}) \quad (2)$$

in which r_0 is the limiting anisotropy at $t=0$, τ_{ri} reflects the rotational relaxation time of either free drug in solution or drug bound to the macrocyclic host and f_i is the relative contribution coming from τ_{ri}. The rotational relaxation of TPT in aqueous solution of pH 6 collected at 530 nm, which is the emission signature of the Z* species, exhibits single exponential decay with a rotational relaxation time of 220 ps. It is already seen from steady-state measurement that a new peak appears at 425 nm (which corresponds to the cationic form of TPT) at the cost of 530 nm on addition of CB[7]. Therefore, we collected anisotropy decays for TPT in the presence of CB[7] at both 530 and 425 nm emission positions to obtain a notion about the rigidity of the surrounding environment sensed by both C* and Z* species, respectively. The anisotropy decay of TPT (C*) bound to CB[7] (collected at 425 nm) yields a retarded rotational relaxation with a relaxation time of approximately 450 ps at 1 mM concentration of CB[7]. This retarded rotational motion of C* in the presence of CB[7] is a further confirmation for the formation of an inclusion complex between CB[7] and the cationic form of TPT. On the other hand, the rotational correlation time of Z* (obtained from collecting the anisotropy decay profile at 530 nm) does not differ much from that for TPT in bulk water even at higher CB[7] concentration (1 mM), thus confirming our conjecture that Z* is not involved in the

inclusion complex formation with CB[7]. However, if Z* interacts with CB[7] by H-bonding interaction (through carbonyl portals), then it is likely that the rotational correlation time of the drug will be unaffected.

The estimated rotational relaxation times τ_r are used to determine the hydrodynamic volumes of inclusion complex formed between TPT and CB[7] by using the following Stokes–Einstein relationship [Eq. (3)]:[22]

$$\tau_r = \frac{1}{6D_r} = \frac{\eta V}{kT} \quad (3)$$

in which D_r and η are the rotational diffusion coefficient and viscosity of the medium, respectively, and V is the hydrodynamic molecular volume of the complex at absolute temperature T. The hydrodynamic diameters calculated from anisotropy data (collected at 425 nm) are found to be 12 and 16 Å for TPT in water and in the presence of 1 mM CB[7], respectively. The calculated hydrodynamic diameter of CB[7] from diffusion measurement is 11.6 Å.[23] Therefore, the increased hydrodynamic diameter of TPT is a proof for the TPT (C form) and CB[7] inclusion complex, which supports our previous interpretations in steady-state, time-resolved studies.

Computational Study

The above experimental findings are further examined with the help of computational studies, as it helps to realise the orientation as well as provide a detailed understanding of the interactions. The TPT:CB[7] inclusion complex was built by bringing TPT (cationic form) and CB[7] close together. Geometry optimisation of the TPT:CB[7] complex was performed at the semi-empirical PM3 level by using Gaussian 09.[24] Here it is pertinent to mention that because the geometry optimisation was performed without consideration of any solvent or other medium parameters, this model provides only a qualitative picture of the complex in the ground state. The optimised structure for the CB[7]:TPT complex is presented in (Figure 5), which clearly shows that the quinoline part of TPT lies partly inside the cavity of CB[7]. Most importantly, the dimethylaminomethylene and hydroxyl groups of the quinoline moiety responsible for zwitterion formation are found to be completely buried inside the CB[7] cavity. As water molecules cannot access these two groups inside the cavity, the excited state of the cationic species (C*) cannot transform to the exited-state zwitterion form (Z*) of TPT in the CB[7]:TPT(C) inclusion complex. Moreover, in this orientation the hydroxyl group of TPT might experience high electron density of carbonyl portals. Therefore, its pK_a may increase if it is encased by the CB[7] nano-cavity. The optimised structure undoubtedly supports the experimental observations and clearly implies that a strong 1:1 ground-state complex is formed between the C form of TPT and CB[7].

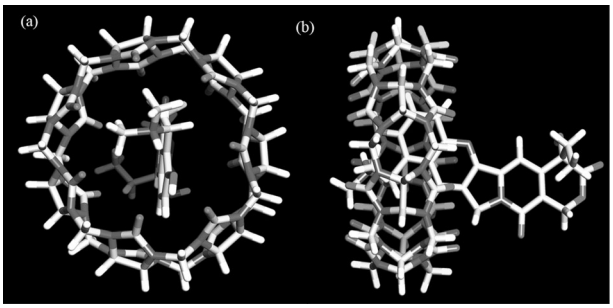

Figure 5. Optimised structure of CB[7]:TPT (1:1) inclusion complex. a) Top view and b) side view.

Salt-Triggered Controlled Release Mechanism of TPT

In most of the drug encapsulation processes release of the drug is immensely important, as it is directly connected to the therapeutic efficacy of the drug.[25] Considering the facts that the cell contains a significant amount of Na^+ ions and cucurbituril portals bind Na^+ with high affinity,[26] we employed NaCl as an external stimulus to affect the non-covalent interaction between the drug and host. On addition of 0.5 M NaCl to the drug-containing 1 mM CB[7] solution, the emission spectra returned to that observed for pH 6.0 aqueous solution (Figure S5). The most prominent feature of the release is obtained from the time-resolved anisotropy measurements, in which it is observed that the NaCl-induced anisotropy decay profile exactly overlays that of TPT in water (Figure 4c). These results clearly manifest that NaCl facilitates the release of the C form of TPT from the CB[7]:TPT(C) inclusion complex. The dominating electrostatic interaction between Na^+ ions and C=O groups at the CB[7] portal may be responsible for the reduced interaction between TPT and CB[7], and ultimately TPT comes out of the cavity.[27] The colour switch from green to blue (for TPT embedded in the CB[7] nano-cavity) and blue to green (its release from CB[7] with the addition of NaCl) is much more interesting, and can be used to monitor the drug-delivery process.

3. Conclusions

We have described the interaction and modulation of the photophysical properties of an important anti-cancer drug, TPT, with CB[7] by several spectroscopic techniques, such as absorption, fluorescence and time-resolved measurements. It was found that CB[7] has a selective affinity to the cationic form (C) of TPT and produces a 1:1 inclusion complex (CB[7]:TPT(C)). The excited-state transformation of C to the zwitterion (Z) form through an ESPT process is restricted inside the CB[7] cavity, which is reflected by the appearance of a new peak at 425 nm at the cost of the 530 nm peak (responsible for the Z form of TPT) in the presence of CB[7]. The appearance of a component at approximately 2 ns in the fluorescence decay profile monitored at 425 nm also confirms the encapsulation of the C form of the drug by the CB[7] host. Moreover, the retarded rotational motion of the C form of TPT fortifies our claim that the C form is encased by the macrocyclic host. On the other hand, the rotational motion of Z* is not hindered in the presence of CB[7], thus indicating that TPT(Z) is not en-

cased by CB[7], but rather it interacts with the C=O portal of CB[7] through hydrogen-bond formation. The process of complexation and molecular orientation of the drug inside the cavity has been conceptualised by using computational studies, which show that the quinoline moiety of TPT lies partly inside the cavity of CB[7], and thereby restricts ESPT and lowers the population of Z*. Finally, controlled release of the drug has been achieved through the introduction of NaCl, which is rich in cells, as an external stimulus. We hope this recognition-mediated binding and release mechanism will be useful for activation of the drug and its controlled release in therapeutic uses.

Experimental Section

TPT and CB[7] were purchased from Sigma–Aldrich and used without further purification. Acetonitrile (MeCN), dimethyl sulfoxide (DMSO), acetone, formamide, methanol, ethanol and dioxane were of high purity (HPLC grade, $>99\%$) and obtained from Spectrochem, India. Millipore water was used for sample preparation. The concentration of TPT in water was adjusted by using the reported value of molar extinction coefficient ($\varepsilon_{381}=25\,580\ \mathrm{M^{-1}\,cm^{-1}}$).[28] CB[7] was added gradually to the solution containing TPT, and the solution was shaken gently after each addition until complete solubilisation of CB[7] took place. Moreover, a 20 min equilibration time was employed for each addition of CB[7].

Absorbance measurements were performed on a PerkinElmer UV–visible spectrophotometer (Lambda-45) and steady-state fluorescence spectra were recorded on a Fluorolog-3 spectrofluorimeter (Horiba Jobin Yvon). All time-resolved fluorescence measurements (both lifetime and anisotropy) were made on a time-correlated single photon counting (TCSPC) spectrometer (Horiba Jobin Yvon IBH, UK). A detailed description of the instrument appears elsewhere.[29] We used a 375 nm diode laser for exciting TPT molecules. The analysis of fluorescence decays was performed by IBH DAS6 analysis software. The quality of each fitting was judged by χ^2 values and the visual inspection of the residuals. The value of $\chi^2 \approx 1$ was considered as the best fit for the plots.

Acknowledgements

This work was partly supported by the Science and Engineering Research Council SERC, the Department of Science and Technology (DST) and the Council of Scientific and Industrial Research (CSIR), Government of India. A.S. is grateful to CSIR for providing a CSIR-Senior Research Fellow (SRF) fellowship and R.K.K. is grateful to the University Grants Commission (UGC) for providing a UGC-Junior Research Fellow (JRF) fellowship. We thank the Director of the Indian Institute of Science Education and Research (IISER) Pune for providing excellent experimental and computation facilities. We are grateful to the anonymous referees for their critical and valuable suggestions.

Keywords: antitumor agents · drug delivery · inclusion compounds · proton transport · supramolecular chemistry

[1] M. E. Wall, M. C. Wani, C. E. Cook, K. H. Palmer, A. T. McPhail, G. A. Sim, *J. Am. Chem. Soc.* **1966**, *88*, 3888.

[2] a) P. D'Arpa, L. F. Liu, *Biochim. Biophys. Acta Rev. Cancer* **1989**, *989*, 163; b) W. D. Kingsbury, J. C. Boehm, D. R. Jakas, K. G. Holden, S. M. Hecht, G. Gallagher, M. J. Caranfa, F. L. McCabe, L. F. Faucette, R. K. Johnson, R. P. Hertzberg, *J. Med. Chem.* **1991**, *34*, 98; c) J. C. Wang, *Annu. Rev. Biochem.* **1996**, *65*, 635; d) Y. Pommier, P. Pourquier, Y. Fan, D. Strumberg, *Biochim. Biophys. Acta Gene Struct. Expression* **1998**, *1400*, 83; e) Y. Pommier, *Nat. Rev. Cancer* **2006**, *6*, 789.

[3] a) B. Anderson, *Gynecol. Oncol.* **1994**, *55*, S143; b) E. K. Rowinsky, A. Adjei, R. C. Donehower, S. D. Gore, R. J. Jones, P. J. Burke, Y. C. Cheng, L. B. Grochow, S. H. Kaufmann, *J. Clin. Oncol.* **1994**, *12*, 2193; c) J. Sehouli, G. Oskay-Özcelik, *Curr. Med. Res. Opin.* **2009**, *25*, 639; d) T. Idris, R. Winter, U. W. E. Lang, E. Petru, *Anticancer Res.* **2009**, *29*, 1761.

[4] a) E. Bardez, A. Chatelain, B. Larrey, B. Valeur, *J. Phys. Chem.* **1994**, *98*, 2357; b) S. A. Strel'tsov, S. L. Grokhovskii, I. A. Kudelina, V. A. Oleinikov, A. L. Zhuze, *Mol. Biol.* **2001**, *35*, 365; c) N. Sanna, G. Chillemi, A. Grandi, S. Castelli, A. Desideri, V. Barone, *J. Am. Chem. Soc.* **2005**, *127*, 15429; d) M. R. di Nunzio, Y. Wang, A. Douhal, *J. Phys. Chem. B* **2012**, *116*, 8182; e) M. R. di Nunzio, Y. Wang, A. Douhal, *J. Phys. Chem. B* **2012**, *116*, 7522.

[5] a) W. J. M. Underberg, R. M. J. Goossen, B. R. Smith, J. H. Beijnen, *J. Pharm. Biomed. Anal.* **1990**, *8*, 681; b) P. Tardi, E. Choice, D. Masin, T. Redelmeier, M. Bally, T. D. Madden, *Cancer Res.* **2000**, *60*, 3389; c) C. Foulon, J. Tedou, T. Queruau Lamerie, C. Vaccher, J. P. Bonte, J. F. Goossens, *Tetrahedron: Asymmetry* **2009**, *20*, 2482; d) G.-S. Wang, H.-Y. Zhang, F. Ding, Y. Liu, *J. Inclusion Phenom. Macrocyclic Chem.* **2011**, *69*, 85.

[6] a) T. G. Burke, Z. H. Mi, *Anal. Biochem.* **1993**, *212*, 285; b) Z. Mi, T. G. Burke, *Biochemistry* **1994**, *33*, 10325; c) Z. Mi, T. G. Burke, *Biochemistry* **1994**, *33*, 12540.

[7] Z. Mi, H. Malak, T. G. Burke, *Biochemistry* **1995**, *34*, 13722.

[8] a) Y.-B. Lim, T. Kim, J. W. Lee, S.-M. Kim, H.-J. Kim, K. Kim, J.-S. Park, *Bioconjugate Chem.* **2002**, *13*, 1181; b) G. Hettiarachchi, D. Nguyen, J. Wu, D. Lucas, D. Ma, L. Isaacs, V. Briken, *PLoS One* **2010**, *5*, e10514; c) V. D. Uzunova, C. Cullinane, K. Brix, W. M. Nau, A. I. Day, *Org. Biomol. Chem.* **2010**, *8*, 2037; d) D. Ma, G. Hettiarachchi, D. Nguyen, B. Zhang, J. B. Wittenberg, P. Y. Zavalij, V. Briken, L. Isaacs, *Nat. Chem.* **2012**, *4*, 503.

[9] a) J. Lagona, P. Mukhopadhyay, S. Chakrabarti, L. Isaacs, *Angew. Chem.* **2005**, *117*, 4922; *Angew. Chem. Int. Ed.* **2005**, *44*, 4844; b) R. N. Dsouza, U. Pischel, W. M. Nau, *Chem. Rev.* **2011**, *111*, 7941; c) W. M. Nau, M. Florea, K. I. Assaf, *Isr. J. Chem.* **2011**, *51*, 559.

[10] a) A. I. Day, R. J. Blanch, A. P. Arnold, S. Lorenzo, G. R. Lewis, I. Dance, *Angew. Chem.* **2002**, *114*, 285; *Angew. Chem. Int. Ed.* **2002**, *41*, 275; b) J. W. Lee, S. Samal, N. Selvapalam, H.-J. Kim, K. Kim, *Acc. Chem. Res.* **2003**, *36*, 621; c) M. F. Czar, R. A. Jockusch, *ChemPhysChem* **2013**, *14*, 1086.

[11] J. Fassberg, V. J. Stella, *J. Pharm. Sci.* **1992**, *81*, 676.

[12] a) I. Chourpa, J.-M. Millot, G. D. Sockalingum, J.-F. Riou, M. Manfait, *Biochim. Biophys. Acta Gen. Subj.* **1998**, *1379*, 353; b) K. M. Solntsev, E. N. Sullivan, L. M. Tolbert, S. Ashkenazi, P. Leiderman, D. Huppert, *J. Am. Chem. Soc.* **2004**, *126*, 12701.

[13] K. Gavvala, A. Sengupta, P. Hazra, *ChemPhysChem* **2013**, *14*, 532.

[14] a) I. Ghosh, W. M. Nau, *Adv. Drug Delivery Rev.* **2012**, *64*, 764; b) R. Wang, L. Yuan, D. H. Macartney, *Chem. Commun.* **2005**, 5867.

[15] C. Reichardt, *Chem. Rev.* **1994**, *94*, 2319.

[16] a) J. V. B. Kanth, H. C. Brown, *J. Org. Chem.* **2001**, *66*, 5359; b) J. García-Alvárez, E. Hevia, A. R. Kennedy, J. Klett, R. E. Mulvey, *Chem. Commun.* **2007**, 2402.

[17] a) J. P. Wignacourt, G. Mairesse, P. Barbier, A. Lorriaux-Rubbens, F. Wallart, *Can. J. Chem.* **1982**, *60*, 1747; b) M. Itoh, T. Adachi, K. Tokumura, *J. Am. Chem. Soc.* **1984**, *106*, 850; c) N. Al-Lawatia, J. Husband, T. Steinbrecher, O. K. Abou-Zied, *J. Phys. Chem. A* **2011**, *115*, 4195.

[18] B. D. Wagner, N. Stojanovic, A. I. Day, R. J. Blanch, *J. Phys. Chem. B* **2003**, *107*, 10741.

[19] a) O. K. Abou-Zied, N. Al-Lawatia, *ChemPhysChem* **2011**, *12*, 270; b) Y. H. Kim, D. W. Cho, S. G. Kang, M. Yoon, D. Kim, *J. Lumin.* **1994**, *59*, 209; c) B. K. Paul, A. Samanta, N. Guchhait, *Langmuir* **2010**, *26*, 3214; d) M. Shaikh, S. Dutta Choudhury, J. Mohanty, A. C. Bhasikuttan, W. M. Nau, H. Pal, *Chem. Eur. J.* **2009**, *15*, 12362.

[20] a) J. R. Lakowicz, *Principles of Fluorescence Spectroscopy, 3rd ed.*, Springer, New York, **2006**; b) M. Y. Berezin, S. Achilefu, *Chem. Rev.* **2010**, *110*, 2641.

[21] a) B. Reija, W. Al-Soufi, M. Novo, J. Vázquez Tato, *J. Phys. Chem. B* **2005**, *109*, 1364; b) M. Shaikh, J. Mohanty, M. Sundararajan, A. C. Bhasikuttan, H. Pal, *J. Phys. Chem. B* **2012**, *116*, 12450.
[22] G. R. Fleming, *Chemical Applications of Ultrafast Spectroscopy*, Oxford University Press, New York, **1986**.
[23] N. J. Wheate, P. G. A. Kumar, A. M. Torres, J. R. Aldrich-Wright, W. S. Price, *J. Phys. Chem. B* **2008**, *112*, 2311.
[24] Gaussian 09 (Revision A.1), M. J. T. Frisch, G. W. Trucks, H. B. Schlegel, G. E. Scuseria, M. A. Robb, J. R. Cheeseman, G. Scalmani, V. Barone, B. Mennucci, G. A. Petersson, H. Nakatsuji, M. Caricato, X. Li, H. P. Hratchian, A. F. Izmaylov, J. Bloino, G. Zheng, J. L. Sonnenberg, M. Hada, M. Ehara, K. Toyota, R. Fukuda, J. Hasegawa, M. Ishida, T. Nakajima, Y. Honda, O. Kitao, H. Nakai, T. Vreven, J. A. Montgomery, Jr., J. E. Peralta, F. Ogliaro, M. Bearpark, J. J. Heyd, E. Brothers, K. N. Kudin, V. N. Staroverov, R. Kobayashi, J. Normand, K. Raghavachari, A. Rendell, J. C. Burant, S. S. Iyengar, J. Tomasi, M. Cossi, N. Rega, J. M. Millam, M. Klene, J. E. Knox, J. B. Cross, V. Bakken, C. Adamo, J. Jaramillo, R. Gomperts, R. E. Stratmann, O. Yazyev, A. J. Austin, R. Cammi, C. Pomelli, J. W. Ochterski, R. L. Martin, K. Morokuma, V. G. Zakrzewski, G. A. Voth, P. Salvador, J. J. Dannenberg, S. Dapprich, A. D. Daniels, Ö. Farkas, J. B. Foresman, J. V. Ortiz, J. Cioslowski, D. Fox, Gaussian, Inc., Wallingford CT, **2009**.
[25] B. Wang, T. J. Siahaan, R. A. Soltero, *Drug Delivery: Principles and Applications*, Wiley-VCH, Weinheim, **2005**.
[26] a) M. Shaikh, J. Mohanty, A. C. Bhasikuttan, V. D. Uzunova, W. M. Nau, H. Pal, *Chem. Commun.* **2008**, 3681; b) H. Tang, D. Fuentealba, Y. H. Ko, N. Selvapalam, K. Kim, C. Bohne, *J. Am. Chem. Soc.* **2011**, *133*, 20623.
[27] J. Mohanty, S. Dutta Choudhury, H. P. Upadhyaya, A. C. Bhasikuttan, H. Pal, *Chem. Eur. J.* **2009**, *15*, 5215.
[28] N. Sanna, G. Chillemi, L. Gontrani, A. Grandi, G. Mancini, S. Castelli, G. Zagotto, C. Zazza, V. Barone, A. Desideri, *J. Phys. Chem. B* **2009**, *113*, 5369.
[29] a) A. Sengupta, R. V. Khade, P. Hazra, *J. Phys. Chem. A* **2011**, *115*, 10398; b) A. Sengupta, W. D. Sasikala, A. Mukherjee, P. Hazra, *ChemPhysChem* **2012**, *13*, 2142; c) K. Gavvala, W. D. Sasikala, A. Sengupta, S. A. Dalvi, A. Mukherjee, P. Hazra, *Phys. Chem. Chem. Phys.* **2013**, *15*, 330.

Received: May 13, 2013
Revised: June 19, 2013
Published online on July 22, 2013